

Leggett's bound and superfluidity in strongly interacting bosons

Lorenzo Pizzino,¹ Haocong Pan,² Thierry Giamarchi,¹ and Hepeng Yao²

¹*DQMP, University of Geneva, 24 Quai Ernest-Ansermet, CH-1211 Geneva, Switzerland*

²*Institute of Quantum Electronics, School of Electronics, Peking University, Beijing 100871, China*

(Dated: December 17, 2025)

A density-based superfluid bound called Leggett's bound has been proved to be a good estimator of the superfluid fraction for cold atomic gases in the mean-field regime. Here, we investigate the accuracy of such bound in the strongly interacting regime, where the mean-field approach fails. Combining quantum Monte Carlo, Gross-Pitaevskii equation and field-theory calculations, we demonstrate that the bound serves as a reliable estimator of the superfluid fraction for strongly interacting bosons at 2D-1D dimensional crossover at low temperatures. By further presenting two counterexamples where the bound predicts trivial results, we shed light on the conditions under which the Leggett's bound serves as a good predictor.

Describing macroscopic quantum phenomena remains one of the central challenges in modern physics. Effects such as superconductivity, Bose-Einstein condensation (BEC), and superfluidity still have many aspects that remain theoretically and experimentally unexplored. A unifying feature of these phenomena is the emergence of collective behavior, encoded in a macroscopic wavefunction, that arises despite complex microscopic interactions [1]. Among them, superfluidity—first observed in 1938 [2, 3] as vanishing viscosity in Helium—offers a particularly striking example. The superfluid fraction f_s quantifies the portion of a system that sustains dissipationless flow and is distinct from the condensate fraction, which measures macroscopic occupation of a single quantum state. While BEC and superfluidity often coexist, especially in weakly interacting systems, they can differ significantly in strongly interacting or low-dimensional settings [4–7].

A significant theoretical advance in quantifying superfluidity was made by A. Leggett, who derived an upper bound for the superfluid fraction in systems with periodic boundary conditions [8]. Using a variational approach and considering the response to a phase twist, he showed that the superfluid fraction along a given direction y satisfies the inequality

$$f_s^y \leq f_{\uparrow,s}^y = \left\langle \frac{n_0}{\langle n(x,y) \rangle_x} \right\rangle_y^{-1} \quad (1)$$

with $n(x,y)$ the local density, n_0 the average total density, x the other direction. The suppression of f_s^y arises from the presence of low-density regions along the x -direction (*transverse nodal surfaces*) which obstruct the current along y . A corresponding heuristic lower bound also exists [9]. These bounds provide an intuitive density-based estimator of superfluidity, independent of detailed wavefunction knowledge. The upper bound has been analyzed in a series of papers and refined to study anisotropic SF [10].

In cold atom experiments, differently from the BEC fraction which is directly measured from the time-of-flight technique, the detection of the superfluid fraction is challenging [11–15]. Various complex methods have been proposed for such measurement, such as laser formed moving obstacle [16], observation of the sound velocity [17, 18] and Josephson effect [19]. Thanks to the quantum gas microscope

technique [20–24], the spatial density distribution of cold atom systems becomes accessible. Therefore, if the Leggett's bound serves as a good estimator for the superfluid fraction, it provides an easy way to probe it.

This question has been extensively investigated in the weakly interacting regime using the Gross-Pitaevskii equation (GPE), which offers access to both ground-state densities and phase structures [18, 25]. By comparing the GPE based theoretical results, the Leggett's bound extracted from the experimental data of density distribution and the superfluid fraction measured from other methods, various groups have validated the bound as a useful proxy for f_s in such regimes. Moreover, under the GPE mean-field scheme, the validity of the bound for other systems has been studied, such as disordered systems [26], BEC mixtures [26], triangular lattice [27] and fermionic systems [28]. This raises key open questions: Can the bound still yield quantitative predictions beyond mean-field regime, such as in strongly interacting systems? How does it behave at finite temperature or near dimensional crossover? Can the Leggett's bound capture more complex behavior and what is the limit of this bound? Addressing these questions requires going beyond GPE and exploring the interplay of interaction, temperature, and dimensionality on the density-based criterion.

In this work, we test the accuracy of Leggett's bound, as a good estimator for the actual superfluid fraction, for strongly interacting bosons in the presence of an optical lattice driving the system from being two-dimensional (2D) to 1D. Combining quantum Monte Carlo (QMC) simulations with GPE solutions, we find the bound to be an excellent SF estimator even in the strong-interacting limit at low temperature, which is beyond the mean-field approximation. In the tight-binding regime, we use field-theory calculations to study the scaling of f_s^y and understand in depth the success of the bound nearby the dimensional crossover point. Moreover, we show two examples where the bound cannot be used as a good estimator showcasing its limitation. We show that the bound accurately predicts the superfluid fraction as long as the mechanism of its variation is correlated to the density modulation of the system.

Model and numerical approach.— The model we consider is described by the 2D Hamiltonian

$$\hat{\mathcal{H}} = \sum_j \left[-\frac{\hbar^2}{2m} \nabla_j^2 + V(\mathbf{r}_j) \right] + \sum_{j < k} U(\mathbf{r}_j - \mathbf{r}_k) \quad (2)$$

where the bosonic particles move under the effect of a periodic potential and the two-body repulsive interaction. We denote with $\mathbf{r} = (x, y)$ the spatial position of the particles, U is the short-range interaction and $V(\mathbf{r}) = V_y \cos^2(ky)$ is the 1D lattice potential along y -direction with $k = \pi/a$ and a is the lattice period. In actual experiment, the interaction strength is determined by the 3D scattering length a_{3D} and the characteristic transverse confinement length l_\perp . They decide the 2D dimensionless coupling constant $\tilde{g}_{2D} = mg_{2D}/\hbar^2$, see details in Refs. [29–31].

In this work, such Hamiltonian is exploited numerically by using Quantum Monte Carlo (QMC) [31, 32] and Gross-Pitaevskii equation (GPE) [33]. From the QMC side, we rely on path integral Monte Carlo in continuous space with worm algorithm implementations [34, 35]. Under the grand-canonical ensemble, we simulate the system at a given interaction strength \tilde{g}_{2D} , temperature T and chemical potential μ . By computing the winding number W_i along the direction $i = x, y$ under periodic boundary conditions, we get the corresponding superfluid fraction f_s^i defined as $f_s^i = m\langle W_i^2 \rangle / \beta \Omega \hbar^2$ with Ω the volume of the system and $\beta = 1/k_B T$ the inverse temperature [36]. We ensure that the selected low-temperature regime gives converged values of $f_s^{i,QMC}$, see Supplemental material for more details. At the same time, by counting the closed worldlines in real space, we also compute the particle density distribution $n(x, y)$ from which we estimate the upper Leggett's bound $f_{\uparrow,s}^{i,QMC}$ by Eq. (1). As we use an unidirectional potential, the density factorizes $n(x, y) = n_0 n(y)$. For this potential, the *strict* upper bound and *putative* lower bound coincide, invalidating the second one as bound. In the remain we consider only the upper bound.

On the other hand, the GPE is expected to work in the limit of weak-interaction where a mean-field approach is valid. We also access the $f_{\uparrow,s}^{i,GPE}$ at zero temperature $k_B T = 0$ by computing the density modulation $n(x, y)$ from the GPE solution similarly as [18]. More precisely, the ground-state properties are governed by

$$\mu \Psi = -\frac{\hbar^2}{2m} \nabla^2 \Psi + V(\mathbf{r}) \Psi + gN|\Psi|^2 \Psi \quad (3)$$

with $\Psi = \Psi(\mathbf{r})$ the Bose field and $g = (\hbar^2/m)\tilde{g}$ the coupling constant. The field is normalized as $\int d^2\mathbf{r}|\Psi(\mathbf{r})|^2 = 1$ and is computed by using the imaginary time evolution [33]. The (dimensionless) parameters are potential amplitude V_y/E_r and the coupling constant gn/E_r with E_r the recoil energy.

Bound's quality beyond mean-field.— We start with exploring the Leggett's bound when interactions are strong such that the mean-field approach is not valid anymore. Indeed, for weak interactions the bound has been successfully exploited,

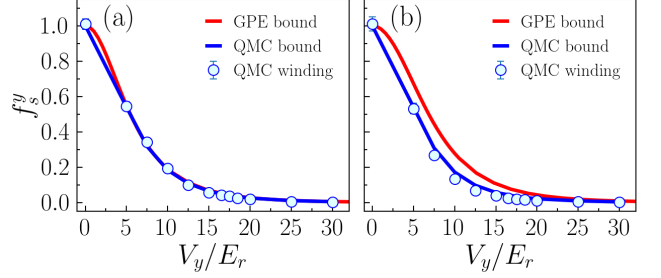


Figure 1. Comparison between the exact superfluid fraction f_s^y via QMC winding number (blue circles) and the Leggett's bound $f_{\uparrow,s}^y$ (solid lines). We use QMC at low temperature $k_B T \simeq 0.005E_r$ and GPE density profiles at zero temperature $k_B T = 0$ (blue and red solid lines, respectively) for varying lattice depths V_y . Panels (a) and (b) correspond to weak ($\tilde{g}_{2D} \simeq 0.018$) and strong ($\tilde{g}_{2D} \simeq 1.364$) interaction regimes, respectively. The QMC bound shows excellent agreement with the exact f_s^y in both cases. As expected, the GPE bound is more accurate in the weak interaction case.

especially by comparing cold atoms experiments with GPE simulations [18, 25, 26]. The results show that the upper bound can be even used to quantitatively estimate the superfluid fraction for weak interaction regime. Here, by using ab initio QMC we are indeed able to go beyond the mean-field regime and test how accurate is the bond in both interaction regimes.

In Fig. 1, we study the bound $f_{\uparrow,s}^y$ in the limit of low temperature as a function of the lattice potential V_y for both weak and strong interactions. We take the temperature $k_B T \simeq 0.005E_r$ where the system is below quantum degeneracy in both 2D and 1D limits. We use QMC and GPE algorithm to extrapolate the density $n(x, y)$ which ranges from being totally flat for $V_y = 0$ to effectively being sliced in 1D chains for very large V_y . Such quantity is then used to compute the upper Leggett's bound $f_{\uparrow,s}^{y,GPE}$ and $f_{\uparrow,s}^{y,QMC}$ from Eq. (1). Both estimators are compared in Fig. 1 with the exact f_s^y computed from the QMC winding number. In both weak (Fig. 1(a)) and strong (Fig. 1(b)) interaction regimes, we observe that the upper bound computed from the QMC particle density not only works as a bound but also seems to be very close to the actual value of f_s^y for the full range of V_y we considered. To our knowledge, this is the first demonstration that the bound also applies as a good estimator in the strong-interacting limit where a mean-field approach would not be suitable. Clearly, for a finite V_y at zero temperature we have a density modulation along the y -direction with a consequent non-zero component of normal fluid and a lower SF fraction f_s^y . This is reflected in the discrepancy of the $f_{\uparrow,s}^{y,GPE}$ with the QMC result, see solid red line in Fig. 1(b). Moreover, for weak interactions, we find the GPE results are also in excellent agreement with QMC as expected, while it overestimates the superfluid fraction in the strongly interacting limit.

Scaling for large V_y .— To further understand the accuracy of Leggett's bound in the strongly interacting regime in

depth, we study the limit of large V_y where the system is well described by a tight-binding model of 1D chains. In this limit, we investigate the system under the Tomonaga-Luttinger liquid (TLL) theory [7]. Compared to the Hamiltonian Eq. (2), which is defined in the continuum, here we account the effect of the transverse coupling in the limit of large V_y [31] by considering instead the hopping term $t_y/E_r = \frac{4}{\sqrt{\pi}}(V_y/E_r)^{3/4}e^{-2\sqrt{V_y/E_r}}$ [37] between nearest neighbors chains along y direction using a variational approach. In this regime, the strong potential confines particles into weakly-coupled tubes, effectively realizing a quasi-1D array.

Following the same footsteps of Ref. [38] (see details in Supplemental material), we compute the free energy within the self-consistent harmonic approximation (SCHA) and use the definition of the superfluid fraction [39] to find

$$f_s^y, \text{SCHA} \sim \frac{d^2 \mathcal{F}_{\text{SCHA}}}{d\Phi^2} \Big|_{\Phi \rightarrow 0} \sim \left(\frac{t_y}{E_r} \right)^{\nu(K)} \quad (4)$$

with the scaling exponent being $\nu(K) = \frac{4K}{4K-1}$ and K the Luttinger parameter ($K = 1$ in the limit of hard-core bosons and $K = 10$ for soft-core bosons) and Φ a small enough flux threading the system: the response of the system to such flux describes its superfluid nature. Given the scaling, the superfluid fraction becomes more sensitive to the interchain coupling t_y/E_r as interactions weaken (increasing K). Moreover, such scaling ν is not affected by finite size [31, 32].

In Fig. 2, we test the SCHA scaling with QMC simulations, which results to be more exact than GPE for the values of interactions we consider, already presented in Fig. 1 but in log-log scale. We consider data that correspond to $f_s^y > 0.005$ and check the scaling exponent according to [31, 32] by fitting in the range $V_y \in [15, 20]E_r$. Starting from the weak-interaction limit in Fig. 2(a), we perform a linear fit which gives a scaling exponent of $\nu_{\text{weak}}^{\text{QMC}} = 1.06 \pm 0.09$ which is in excellent agreement with $\nu(K = 10) \simeq 1.03$. On the other hand, the bound gives a scaling of $\nu_{\text{weak}}^{\text{QMC bound}} = 0.96 \pm 0.01$. We thus see that although the two results agree very well quantitatively as shown in Fig. 2(a), the bound and the full calculation indicate different scalings as a function of t_y . The bound will thus become more and more inaccurate as $t_y \rightarrow 0$. This is due to the quantum effects coming from the interactions that cannot be captured by a density description alone. However for weak couplings the exponents are so close that it would require abysmally small t_y to have a sizeable difference. The bound is thus a remarkable estimator in practice for all reasonable values of t_y as shown in Fig. 2(a)

This trend becomes more obvious for the strongly interacting case shown in Fig. 2(b). The winding number fit gives a scaling exponent of $\nu_{\text{strong}}^{\text{QMC}} = 1.33 \pm 0.07$ which is again in excellent agreement with the field-theory prediction $\nu(K = 1) = 4/3$. At the same time, compared to the bound, the scaling exponent we find is $\nu_{\text{strong}}^{\text{QMC bound}} = 1.00 \pm 0.03$. Therefore, for strong interactions the bound is unable to predict the correct scaling, contrarily to the case of weak inter-

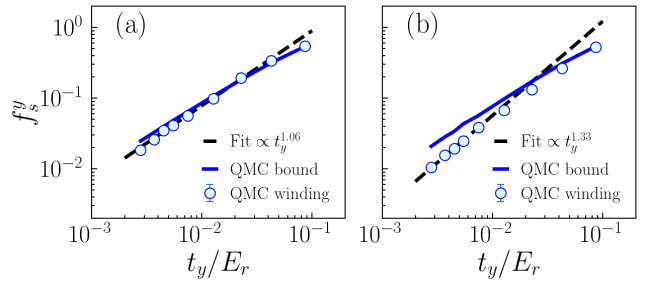


Figure 2. Scaling analysis of f_s^y for small t_y from QMC data. Panels (a) and (b) correspond to weak ($\tilde{g}_{2D} \simeq 0.018$) and strong ($\tilde{g}_{2D} \simeq 1.364$) interaction regimes, respectively, for a system size of $L_x = 25a$, $L_y = 10a$ and $k_B T \simeq 0.005E_r$. The black dashed lines are linear fits for small t_y of the exact SF fraction computed with QMC winding number (light blue circles) and the blue solid line is the QMC bound. We find the scaling exponents to be in excellent agreement with the SCHA predictions $\nu(K) = \frac{4K}{4K-1}$. For weak interactions ($K = 10$) we have $\nu_{\text{weak}}^{\text{QMC}} = 1.06 \pm 0.09$ and for strong interactions ($K = 1$) we find $\nu_{\text{strong}}^{\text{QMC}} = 1.33 \pm 0.07$. Fitting the QMC bounds, we have $\nu_{\text{weak}}^{\text{QMC bound}} = 0.96 \pm 0.01$ and $\nu_{\text{strong}}^{\text{QMC bound}} = 1.00 \pm 0.03$.

actions, even though the discrepancy between the QMC and bound is not dramatic. This result shows that the density itself is insufficient to infer on the effect of interactions on the system. Furthermore, as we move towards 1D geometry, the effect of quantum fluctuations are enhanced and even for an *almost* constant density the bound predicts trivial results. Indeed, the ratio between the winding number and bound suggests that the bound becomes increasingly more incorrect for small t_y .

Two special cases where the bound strongly overestimates the superfluid fraction.— So far we have shown how the Leggett's bound behaves as a good estimator for the superfluid fraction of low temperature systems as a function of interactions. Here, we want to further demonstrate that it is not always the case by presenting two counter examples. Firstly, we explore the dimensional crossover at intermediate temperature regime with $\tilde{g}_{2D} = 1.36$ and $k_B T = 0.09E_r$. At this temperature, the system is a 2D superfluid, but becomes a normal fluid when it enters 1D regime (increasing V_y). Therefore, the longitudinal superfluid fraction f_s^x will decrease as a function of V_y according to Ref. [31]. In Fig. 3(a1), we compute the f_s^x from the winding number as V_y (light blue balls). Clearly, we see that f_s^x decreases with V_y as expected. However, by plotting the density profile along x -direction in Fig. 3(a2), we find the absence of density modulation which leads to a constant upper bound, see black solid line in Fig. 3(a1). This is due to the fact that the decrease of f_s^x is caused by the joint effect of thermal and quantum fluctuations along the longitudinal directions, which does not necessarily reflect on the density profile. Therefore, the computed bound cannot encode such information and is unable to follow the variation of superfluid fraction.

As a second example, we start off with a large potential V_y by forcing the system to be in the 1D limit (large V_y) at low temperature. We now have to recall that for purely 1D systems in strong interaction regime, an arbitrarily weak periodic lattice potential can localize particle and destroy even at zero temperature a finite SF fraction, known as the pinning Mott transition [40–43]. From the bound’s perspective, such a potential only mildly affects the density modulation and therefore can potentially lead the bound to give a trivial result. We show in Fig. 3(b1) the Mott transition in such a shallow lattice case. Here, the potential along x-direction writes $V(x) = V_x \cos^2(kx)$ with $k = \pi/a$. More precisely, we take the parameters $\tilde{g}_{1D} = 7$ and $V_x = 2E_r$, with a temperature of $k_B T \simeq 0.004E_r$ and plot f_s^x as a function of the chemical potential μ around the Mott lobe $na = 1$. The transition point is located in the window $\mu_{c1} = 1.38E_r$ and $\mu_{c2} = 1.51E_r$, and within the range $\mu_{c1} < \mu < \mu_{c2}$ the superfluid fraction f_s^x vanishes. However, such a small oscillating potential $V_x = 2E_r$ only causes a weak modulation on the corresponding density profile. In Fig. 3(b2), we show one example of the density profile for $\mu = 1.45E_r$ in the center of the Mott lobe. Clearly, it only oscillates between $na \simeq 0.48$ and $na \simeq 1.65$ without touching zero. As a consequence, the corresponding Leggett’s bound gives a large value $f_{\uparrow,s}^x \simeq 0.827$. In fact, in the full range of μ we considered, the Leggett’s bound is not sensitive to μ and shows almost a constant, see blue solid line in Fig. 3(b1). Hence, the density modulation is one of the ingredients to suppress SF but not the only one: if more subtle mechanisms are involved, then the upper bound usually gives trivial results as shown in this section.

Conclusion and experimental observability.— In this paper, we shed light on the conditions under which the Leggett’s bound serves as a good estimator for superfluid fraction of strongly interacting bosons. For bosonic systems at 2D-1D dimensional crossover and low temperature, we find the bound is an accurate estimator of the transverse superfluidity for both strong and weak interaction regimes. While the weak interaction limit was already widely studied, we get further insights from the SCHA scaling on the strong interaction limit. The results confirm that the bound scaling agrees with QMC and SCHA in the limit of weak-interactions, while the discrepancy becomes larger for strong-interactions. Therefore, we conclude that the bound serves as a quantitative superfluid estimator regardless of the value of interactions but is not able to fully predict the effect of interactions in the limit of quasi-1D. We further show two additional cases where the bound *fails* to be a good superfluid estimator, namely the dimensional crossover at higher temperature and the pinning Mott transition in 1D Tonks-Girardeau regime. In both cases, the density is weakly modulated and we find $f_{\uparrow,s}^x \sim 1$. We conclude that the bound is an extremely powerful tool to study the superfluid fraction when the superfluid suppression mechanism is linked to density modulation. Effects like thermal fluctuations and interferences can also cause changes on superfluid fraction while making less influence on the density, which make the bound less powerful. We recall that the exam-

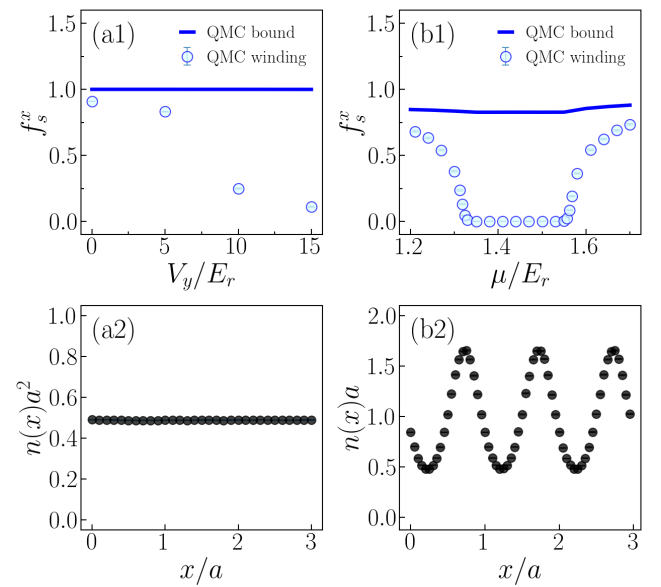


Figure 3. Two cases where the bound is no more a quantitative SF estimator (solid line). In panel (a1) we study the longitudinal SF fraction f_s^x at intermediate temperature $k_B T = 0.09E_r$ and strong interactions $\tilde{g}_{2D} \simeq 1.364$ with system size of $L_x = L_y = 12a$. (a2) shows the corresponded density profile $n(x)$ for the case $V_y = 10E_r$. It leads to the constant bound (blue solid curve in (a1) which is not compatible with the f_s^x (light blue balls). In panel (b1) we consider large enough V_y such that the system is strictly 1D. We further consider small $V_x = 2E_r$ in the Tonks-Girardeau limit, with the 1D dimensionless coupling constant $\tilde{g}_{1D} = 7$ and temperature $k_B T \simeq 0.004E_r$ and system sizes $L_x = 50a$. The system shows a transition from 1D superfluid state to 1D Mott insulator state by plotting the superfluid fraction f_s^x as a function of the chemical potential μ . We show the results from both the QMC winding (light blue balls) and Leggett’s bound (blue solid curve). In panel (b2) we present one example of the density profile $n(x)$ at $\mu = 1.45E_r$.

ples we presented are intimately linked with the peculiar case of 1D quantum systems. Such a scenario is more difficult to occur in 2D or 3D where, unless we have finite range interactions or disorder [26], the localization (density modulations) can be indeed externally imposed with non-trivial lattices [44] or self-induced (supersolids).

Concerning nowadays cold atom experiments, we stress out that such tool is very useful, especially for situations where the density profile is easy to obtain. For instance, single-site resolution imaging via quantum gas microscopes [20–24] provides direct access to the density profile, making Leggett’s bound particularly appealing as an indirect probe of superfluidity. Moreover, on the theoretical side, it would be interesting to study the validity of the bound for strongly interacting bosons in more complex potentials, such as speckle or quasiperiodic potentials. Also, it is interesting to explore the bound in case of fermionic particles which could present a different physical scenario compared to the bosonic case.

We thank Pietro Massignan, Jean Dalibard, Sandro Stringari and Grigory Astrakharchik for fruitful discussions

and useful comments. We thank Wayne Saslow for useful comments and making us aware of relevant papers on the subject of Leggett's bounds. T.G. thanks the Institut Henri Poincaré (UAR 839 CNRS-Sorbonne Université). This work is supported by the Swiss National Science Foundation under grant number 200020-219400 and The Fundamental Research Funds for the Central Universities, Peking University. Numerical calculations make use of the ALPS scheduler library and statistical analysis tools [45–47].

[1] L. Pitaevskii and S. Stringari, *Bose-Einstein condensation and superfluidity*, Vol. 164 (Oxford University Press, 2016).

[2] J. F. Allen and A. D. Misener, Flow of liquid helium ii., *Nature* **141**, 75 (1938).

[3] P. Kapitza, Viscosity of liquid helium below the λ point., *Nature* **141**, 74 (1938).

[4] V. L. Berezinskii, Sov. Phys. JETP **34**, 610 (1972).

[5] J. M. Kosterlitz and D. J. D J Thouless, Ordering, metastability and phase transitions in two-dimensional systems, *J. Phys. C: Solid State Phys.* **6**, 1181 (1973).

[6] Z. Hadzibabic and J. Dalibard, Two-dimensional bose fluids: An atomic physics perspective, *La Rivista del Nuovo Cimento* **34**, 389 (2011).

[7] T. Giamarchi, *Quantum Physics in One Dimension*, International series of monographs on physics, Vol. 121 (Oxford University Press, Oxford, 2004).

[8] A. J. Leggett, Can a solid be "superfluid"?, *Phys. Rev. Lett.* **25**, 1543 (1970).

[9] A. Leggett, On the superfluid fraction of an arbitrary many-body system at $T=0$, *Journal of statistical physics* **93**, 927 (1998).

[10] W. M. Saslow, Superfluidity of periodic solids, *Phys. Rev. Lett.* **36**, 1151 (1976).

[11] K. B. Davis, M. O. Mewes, M. R. Andrews, N. J. Van Druten, D. S. Durfee, D. M. Kurn, and W. Ketterle, Bose-Einstein condensation in a gas of sodium atoms, *Phys. Rev. Lett.* **75**, 3969 (1995).

[12] S. Richard, F. Gerbier, J. Thywissen, M. Hugbart, P. Bouyer, and A. Aspect, Momentum spectroscopy of 1D phase fluctuations in Bose-Einstein condensates, *Phys. Rev. Lett.* **91**, 010405 (2003).

[13] T. Stöferle, H. Moritz, C. Schori, M. Köhl, and T. Esslinger, Transition from a strongly interacting 1d superfluid to a mott insulator, *Phys. Rev. Lett.* **92**, 130403 (2004).

[14] F. Gerbier, A. Widera, S. Fölling, O. Mandel, T. Gericke, and I. Bloch, Phase coherence of an atomic Mott insulator, arXiv e-print **cond-mat**, 0503452 (2005).

[15] Y. Guo, H. Yao, S. Ramanjanappa, S. Dhar, M. Horvath, L. Pizzino, T. Giamarchi, M. Landini, and H.-C. Nägerl, Observation of the 2d-1d crossover in strongly interacting ultracold bosons, *Nature Physics* **20**, 934 (2024).

[16] R. Desbuquois, L. Chomaz, T. Yefsah, J. Léonard, J. Beugnon, C. Weitenberg, and J. Dalibard, Superfluid behaviour of a two-dimensional Bose gases, *Nat. Phys.* **8**, 645 (2012).

[17] P. Christodoulou, M. Gałka, N. Dogra, R. Lopes, J. Schmitt, and Z. Hadzibabic, Observation of first and second sound in a BKT superfluid, *Nature (London)* **594**, 191 (2021).

[18] G. Chauveau, C. Maury, F. Rabec, C. Heintze, G. Brochier, S. Nascimbene, J. Dalibard, J. Beugnon, S. M. Roccuzzo, and S. Stringari, Superfluid fraction in an interacting spatially modulated bose-einstein condensate, *Phys. Rev. Lett.* **130**, 226003 (2023).

[19] G. Biagioni, N. Antolini, B. Donelli, L. Pezzè, A. Smerzi, M. Fattori, A. Fioretti, C. Gabbanini, M. Inguscio, L. Tanzi, and G. Modugno, Measurement of the superfluid fraction of a supersolid by josephson effect, *Nature* **629**, 773 (2024).

[20] W. S. Bakr, J. I. Gillen, A. Peng, S. Fölling, and M. Greiner, A quantum gas microscope for detecting single atoms in a Hubbard-regime optical lattice, *Nature (London)* **462**, 74 (2009).

[21] C. Weitenberg, P. Schauß, T. Fukuhara, M. Cheneau, M. Endres, I. Bloch, and S. Kuhr, Coherent light scattering from a two-dimensional Mott insulator, *Phys. Rev. Lett.* **106**, 215301 (2011).

[22] M. Cheneau, P. Barmettler, D. Poletti, M. Endres, P. Schauß, T. Fukuhara, C. Gross, I. Bloch, C. Kollath, and S. Kuhr, Light-cone-like spreading of correlations in a quantum many-body system, *Nature (London)* **481**, 484 (2012).

[23] D. Greif, M. F. Parsons, A. Mazurenko, C. S. Chiu, S. Blatt, F. Huber, G. Ji, , and M. Greiner, Site-resolved imaging of a fermionic Mott insulator, *Science* **351**, 953 (2016).

[24] E. Haller, J. Hudson, A. Kelly, D. A. Cotta, B. Peaudecerf, G. D. Bruce, and S. Kuhr, Single-atom imaging of fermions in a quantum-gas microscope, *Nat. Phys.* **1**, 738 (2015).

[25] J. Tao, M. Zhao, and I. B. Spielman, Observation of anisotropic superfluid density in an artificial crystal, *Phys. Rev. Lett.* **131**, 163401 (2023).

[26] D. Pérez-Cruz, G. E. Astrakharchik, and P. Massignan, Superfluid fraction of interacting bosonic gases, *Phys. Rev. A* **111**, L011302 (2025).

[27] F. Rabec, G. Brochier, S. Wattellier, G. Chauveau, Y. Li, S. Nascimbene, J. Dalibard, and J. Beugnon, Superfluid fraction of a 2d bose-einstein condensate in a triangular lattice (2025), arXiv:2511.04575 [cond-mat.quant-gas].

[28] G. Orso and S. Stringari, Superfluid fraction and leggett bound in a density-modulated strongly interacting fermi gas at zero temperature, *Phys. Rev. A* **109**, 023301 (2024).

[29] D. Petrov, M. Holzmann, and G. Shlyapnikov, Bose-Einstein condensation in quasi-2D trapped gases, *Phys. Rev. Lett.* **84**, 2551 (2000).

[30] D. Petrov and G. Shlyapnikov, Interatomic collisions in a tightly confined Bose gas, *Phys. Rev. A* **64**, 012706 (2001).

[31] H. Yao, L. Pizzino, and T. Giamarchi, Strongly-interacting bosons at 2D-1D dimensional crossover, *SciPost Phys.* **15**, 050 (2023).

[32] L. Pizzino, H. Yao, and T. Giamarchi, Finite size analysis for interacting bosons at the one-two dimensional crossover, *Phys. Rev. Res.* **7**, 013021 (2025).

[33] R. Gautier, H. Yao, and L. Sanchez-Palencia, Strongly interacting bosons in a two-dimensional quasicrystal lattice, *Phys. Rev. Lett.* **126**, 110401 (2021).

[34] M. Boninsegni, N. Prokof'ev, and B. Svistunov, Worm algorithm for continuous-space path integral Monte Carlo simulations, *Phys. Rev. Lett.* **96**, 070601 (2006).

[35] M. Boninsegni, N. V. Prokof'ev, and B. V. Svistunov, Worm algorithm and diagrammatic Monte Carlo: A new approach to continuous-space path integral Monte Carlo simulations, *Phys. Rev. E* **74**, 036701 (2006).

[36] D. M. Ceperley, Path integrals in the theory of condensed helium, *Rev. Mod. Phys.* **67**, 279 (1995).

[37] I. Bloch, J. Dalibard, and W. Zwerger, Many-body physics with ultracold gases, *Rev. Mod. Phys.* **80**, 885 (2008).

[38] M. Cazalilla, A. Ho, and T. Giamarchi, Interacting bose gases in

quasi-one-dimensional optical lattices, *New Journal of Physics* **8**, 158 (2006).

[39] M. E. Fisher, M. N. Barber, and D. Jasnow, Helicity modulus, superfluidity, and scaling in isotropic systems, *Phys. Rev. A* **8**, 1111 (1973).

[40] E. Haller, R. Hart, M. J. Mark, J. G. Danzl, L. Reichsöllner, M. Gustavsson, M. Dalmonte, G. Pupillo, and H.-C. Nägerl, Pinning quantum phase transition for a Luttinger liquid of strongly interacting bosons, *Nature (London)* **466**, 597 (2010).

[41] G. Boéris, L. Gori, M. D. Hoogerland, A. Kumar, E. Lucioni, L. Tanzi, M. Inguscio, T. Giamarchi, C. D'Errico, G. Carleo, G. Modugno, and L. Sanchez-Palencia, Mott transition for strongly interacting one-dimensional bosons in a shallow periodic potential, *Phys. Rev. A* **93**, 011601(R) (2016).

[42] H. Yao, T. Giamarchi, and L. Sanchez-Palencia, Lieb-Liniger bosons in a shallow quasiperiodic potential: Bose glass phase and fractal Mott lobes, *Phys. Rev. Lett.* **125**, 060401 (2020).

[43] H. Yao, L. Tanzi, L. Sanchez-Palencia, T. Giamarchi, G. Modugno, and C. D'Errico, Mott transition for a lieb-liniger gas in a shallow quasiperiodic potential: Delocalization induced by disorder, *Phys. Rev. Lett.* **133**, 123401 (2024).

[44] F. Rabec, G. Brochier, S. Wattellier, G. Chauveau, Y. Li, S. Nascimbene, J. Dalibard, and J. Beugnon, Superfluid fraction of a 2d bose-einstein condensate in a triangular lattice (2025), arXiv:2511.04575 [cond-mat.quant-gas].

[45] M. Troyer, B. Ammon, and E. Heeb, Parallel object oriented Monte Carlo simulations, *Lect. Notes Comput. Sci.* **1505**, 191 (1998).

[46] A. Albuquerque, F. Alet, P. Corboz, P. Dayal, A. Feiguin, S. Fuchs, L. Gamper, E. Gull, S. Guertler, A. Honecker, R. Igarashi, M. Koerner, A. Kozhevnikov, A. Laeuchli, S. Manmana, M. Matsumoto, I. McCulloch, F. Michel, R. Noack, G. Pawłowski, L. Pollet, T. Pruschke, U. Schollwöck, S. Todo, S. Trebst, M. Troyer, P. Werner, and S. Wessel, The ALPS project release 1.3: Open-source software for strongly correlated systems, *J. Magn. Magn. Mater.* **310**, 1187 (2007).

[47] B. Bauer, L. D. Carr, H. G. Evertz, A. Feiguin, J. Freire, S. Fuchs, L. Gamper, J. Gukelberger, E. Gull, S. Guertler, A. Hehn, R. Igarashi, S. V. Isakov, D. Koop, P. N. Ma, P. Mates, H. Matsuo, O. Parcollet, G. Pawłowski, J. D. Picon, L. Pollet, E. Santos, V. W. Scarola, U. Schollwöck, C. Silva, B. Surer, S. Todo, S. Trebst, M. Troyer, M. L. Wall, P. Werner, and S. Wessel, The alps project release 2.0: open source software for strongly correlated systems, *J. Stat. Mech.: Theory Exp.* **2011** (05), P05001.

[48] M. Olshanii, Atomic scattering in the presence of an external confinement and a gas of impenetrable bosons, *Phys. Rev. Lett.* **81**, 938 (1998).

[49] M. A. Cazalilla, R. Citro, T. Giamarchi, E. Orignac, and M. Rigol, One dimensional bosons: From condensed matter systems to ultracold gases, *Rev. Mod. Phys.* **83**, 1405 (2011).

Supplemental Material for

Leggett's bound and superfluidity in strongly-interacting bosons

In this supplemental material, we provide complementary details regarding the analytic and numerical results presented in the manuscript.

S1. S1. SUPERFLUID FRACTION SCALING FROM VARIATIONAL METHOD

In this section, we show how to find the superfluid fraction along the y -direction in the limit of 1D coupled chains by using a field-theory approach. We start off by the single-particle operator which in the bosonization dictionary reads $\psi(x) = \sqrt{A_B \rho_0} e^{i\theta(x)}$ with A_B a non-universal model-dependent pre-factor and ρ_0 the density of particles. Here, θ is the field corresponding to the phase of the bosonic particles. The action of the coupled chains is

$$\mathcal{S} = \mathcal{S}_0 - A_B \rho_0 t_y \sum_{\langle i,j \rangle} \int dx d\tau \cos(\theta_i(x, \tau) - \theta_j(x, \tau)) \quad (S1)$$

with \mathcal{S}_0 being the action of the single-chain and the second term generated by the very weak transverse coupling. In our notation, x is the (longitudinal) spatial coordinate and τ the imaginary time coordinate while $\langle i, j \rangle$ denote n.n. chains indices.

In order to compute f_s^y , we perform a gauge transformation along the y -direction such that $\theta_j(x, \tau) \rightarrow \theta_j(x, \tau) + \Phi j$ and therefore we modify the argument of the cosine while \mathcal{S}_0 remains unchanged. We denote with Φ a small flux threading the system. Next, in the limit of small temperature (small fluctuations) we consider the contribution coming from small oscillations of the cosine which results in having an effective action of the form

$$\begin{aligned} \mathcal{S} &= \mathcal{S}_0 - A_B \rho_0 \tilde{t}_y \sum_{\langle i,j \rangle} \int dx d\tau \left[1 - \frac{1}{2} \left((\theta_i(x, \tau) - \theta_j(x, \tau))^2 + \Phi^2 \right) \right] \\ &= \mathcal{S}_0 + \frac{A_B \rho_0 \tilde{t}_y}{2} \sum_{\langle i,j \rangle} \int dx d\tau (\theta_i(x, \tau) - \theta_j(x, \tau))^2 + \frac{A_B \rho_0 \tilde{t}_y}{2} \frac{L_y z}{2} L_x \beta \Phi^2 + \text{const} \end{aligned} \quad (S2)$$

where \tilde{t}_y has to be found self-consistently and has a known scaling of $\tilde{t}_y \sim t_y^{\frac{4K}{4K-1}}$ [38]. It's of our interest to keep track of the Φ^2 term. The factor $\frac{L_y z}{2}$ comes from counting the number of n.n. along the y -direction, β is the inverse temperature and L_x is the system size along the longitudinal direction. From the action, we have access to the partition function which allows us to compute the free energy as

$$\mathcal{F} = -k_B T \ln \left[e^{-\frac{1}{4} A_B z \rho_0 \tilde{t}_y L_y L_x \beta \Phi^2} \int \mathcal{D}\theta^* \int \mathcal{D}\theta e^{-\frac{1}{2\beta L_y} \sum_{\mathbf{Q}} [\dots] \theta_{\mathbf{Q}}^* \theta_{\mathbf{Q}}} \right] \sim \frac{1}{4} A_B z \rho_0 \tilde{t}_y L_y L_x \Phi^2 \quad (S3)$$

and the superfluid fraction reads

$$f_s^y \sim \frac{d^2 \mathcal{F}}{d\Phi^2} \sim \tilde{t}_y \sim t_y^{\frac{4K}{4K-1}} \quad (S4)$$

which gives the power-law scaling as a function of the Luttinger parameter K .

S2. S2. QUANTUM MONTE CARLO CALCULATIONS

The calculations of superfluid fraction and its upper bound in the main paper highly rely on one type of quantum Monte Carlo (QMC) calculations, namely path integral Monte Carlo implemented with worm algorithm [34, 35]. Thanks to the open worldline configurations in worm algorithm, we work under the grand canonical ensemble. Given temperature T , 2D scattering length a_{2D} and chemical potential μ , relevant observables that we are interested in are computable. In this section, we provide more details about the QMC calculations.

A. Computation of superfluid fraction

We further compute the superfluid fraction f_s^x or f_s^y and their upper bounds $f_{\uparrow,s}^x$ or $f_{\uparrow,s}^y$ from two different methods, respectively. On one hand, we perform the winding method under periodic boundary conditions. More specifically, the definition of superfluid mass along certain direction i is

$$M_s^i = M - \frac{\partial \langle \hat{P}_i \rangle}{\partial v}, \quad (\text{S5})$$

where v is the velocity with respect to the reference frame, M the mass of the system, and \hat{P}_i the momentum operator of the system along certain direction i , where $i = x, y$. Then, the superfluid density can be written as $n_s^i = M_s^i / mL_x L_y$, where m is the mass of a single particle. Recalling that the thermodynamic averages of an observable \hat{A} can be estimated by

$$\langle \hat{A} \rangle = \frac{\text{Tr} \left[e^{-\beta(\mathcal{H}-\mu\hat{N})} \hat{A} \right]}{\text{Tr} \left[e^{-\beta(\mathcal{H}-\mu\hat{N})} \right]}, \quad (\text{S6})$$

where \mathcal{H} is the Hamiltonian, \hat{N} the number of particles operator, $\beta = 1/k_B T$ the energy scale of inverse temperature, and Tr the trace operator [36]. By inserting $\hat{A} = \hat{P}_i$ and $\mathcal{H} = \hat{H}_v = \hat{H} - \mathbf{v} \cdot \hat{\mathbf{P}}$, we have

$$n_s^i = n_0 - \frac{m}{L_x L_y} \int_0^\beta d\tau \langle \hat{P}_i(\tau) \hat{P}_i(0) \rangle, \quad (\text{S7})$$

where n_0 is the average total density.

To calculate the correlator $\langle \hat{P}_i(\tau) \hat{P}_i(0) \rangle$ in the integral, we replace the integral \int_0^β by the discrete sum $\epsilon \sum_{j=0}^{J-1}$ by slicing the imaginary time space into J small time step ϵ , such that $\epsilon = \beta/J$. Then, we take $\epsilon \rightarrow 0$ and obtain

$$n_s^i = \frac{1}{\beta L_x L_y} \frac{m}{\hbar^2} \langle W_i^2 \rangle, \quad i = x, y, \quad (\text{S8})$$

with W_i the winding number along i direction under the periodical boundary conditions. Finally, we can further obtain the superfluid fraction by $f_s^i = n_s^i / n_0$, $i = x, y$, with

$$n_0 = \frac{1}{L_x L_y} \langle \hat{N} \rangle, \quad (\text{S9})$$

where the particle number $\langle \hat{N} \rangle$ can be directly obtained by counting the number of worldlines.

On the other hand, the upper bound of the superfluid fraction is linked to the density profile by a concise formula, namely Eq. (1) of the main text[8, 18]. Since the local density is diagonal in the position representation, and using the translational invariance in the imaginary time of the path integral configurations, we can calculate the density distribution $n(\mathbf{r})$ in the simulation as

$$n(\mathbf{r}) = \frac{1}{J} \left\langle \sum_{j=1}^{J-1} \sum_{i=0}^N \delta(\mathbf{r} - \mathbf{r}_i^j) \right\rangle, \quad (\text{S10})$$

where the superscript of \mathbf{r} represents the number of steps in the imaginary time evolution and the subscript represents the label of a certain particle. With the computed $n(\mathbf{r})$, we can then further compute the upper bound f_s^i according to Eq. (1) of the main text.

B. Depiction of interaction

In the QMC calculations, we use the Trotter-Suzuki approximation for estimating the short-time propagator, and only consider two-body interaction under pair-product approximation, where a generalized 2D interaction propagator that can work for any interaction regime is generated, similarly as Ref. [33].

When we use a strong harmonic confinement ω_\perp on the transverse direction to generate a 2D gas, the 2D scattering length a_{2D} can be expressed as a function of the 3D scattering length a_{3D} and characteristic transverse length $l_\perp = \sqrt{\hbar/m\omega_\perp}$ [29, 30],

which writes $a_{2D} \simeq 2.092l_{\perp} \exp\left(-\sqrt{\pi/2}l_{\perp}/a_{3D}\right)$. For 2D or 1D cases, we can link the scattering length with 2D coupling constant g_{2D} or 1D coupling constant g_{1D} , which describe the pseudo-potential strength [37]. The 2D coupling constant g_{2D} can be written as [29, 30]

$$\tilde{g}_{2D} \simeq \frac{4\pi}{2 \ln(a/a_{2D}) + \ln(\Lambda E_r/\mu)}, \quad (S11)$$

with $\Lambda \simeq 2.092^2/\pi^3 \simeq 0.141$, $E_r = \pi^2\hbar^2/2ma^2$ the recoil energy, and $\tilde{g}_{2D} = mg_{2D}/\hbar^2$. The 1D coupling constant g_{1D} can be written as [37, 48].

$$\tilde{g}_{1D} = \frac{2a_{3D}}{l_{\perp}^2} \left(1 - \frac{1.036a_{3D}}{l_{\perp}}\right)^{-1}, \quad (S12)$$

with $\tilde{g}_{1D} = mg_{1D}/\hbar^2$. The definition we used here is the same as the one in Ref. [31].

In this paper, we consider $a_{2D} = 10^{-150}a$ for 2D weak interactions and $a_{2D} = 0.01a$ for 2D strong interactions, where a is the lattice period, and particle density $n = N/L_xL_y = 0.5a^{-2}$, which is satisfied by choosing proper chemical potential μ . Since the condition $a/a_{2D} \gg \Lambda E_r/\mu$ is satisfied in both 2D weak and strong interactions, the 2D dimensionless coupling constant can be reduced to $\tilde{g}_{2D} \simeq 2\pi/\ln(a/a_{2D})$, which gives $\tilde{g}_{2D} \simeq 0.018$ for 2D weak interactions and $\tilde{g}_{2D} \simeq 1.364$ for 2D strong interactions. Notably, the criteria of strongly-interacting bosons is $\gamma_{2D} = \tilde{g}_{2D} \gtrsim 1$, see Refs. [6, 37, 49]. For the strictly-1D calculation in Fig. 3 (b) of the main text, we consider the 1D dimensionless coupling constant $\tilde{g}_{1D} = 7$. For particle density around $na = 1$, it leads to the Lieb-Liniger parameter $\gamma_{1D} = \tilde{g}_{1D}/na = 7$, which also satisfies the criteria of strong interaction regime $\gamma_{1D} \gg 1$.

C. Numerical parameters and validity of approximations

Here, we provide the numerical parameters we choose, which ensure the validity of approximations and minimizes the numerical errors.

For the imaginary time space discretization, we use small imaginary time steps $\epsilon = 0.01 - 0.02E_r^{-1}$ and $\epsilon = 0.05E_r^{-1}$ for the 2D and 1D cases, respectively. Both of them enable us to use the Trotter-Suzuki approximation and the pair-product approximation by meeting the criteria $\epsilon \ll \beta$ and $\sigma = \sqrt{\hbar^2\epsilon/m} \ll a$, where σ is the corresponding standard deviation of the free particle propagator.

Besides, a sufficiently large number of warm-up steps and sampling iterations are needed to guarantee the adequacy of the Monte Carlo statistics. For the 2D cases, we take 10^8 warm-up steps for most of the data points, with $\sim 10^7$ iterations for both strong and weak interactions. For the 1D cases, we take 10^6 each for warm-up steps and iterations. Finally, we have made sure that a larger number of warm-up steps and sampling iterations will not change any physics presented in the main paper.

D. Convergence of superfluid fraction for small temperatures

In the main text, for all the QMC calculations in Figs. 1 and 2, we always use the temperature $k_B T = 0.005E_r$. We assume this temperature is low enough such that there is no finite-temperature effect in the obtained results. Here, we examine this point by computing the superfluid fraction at various temperatures for the strong interaction case, where a deviation between the Leggett's bound and the winding superfluid fraction is observed.

As shown in Fig. S1, on top of the results in Fig. 2 (b) of the main text, we further examine the cases of a lower temperature $k_B T = 0.0034E_r$ and a higher temperature $k_B T = 0.01E_r$ under strong interaction at $V_y/E_r = 5, 10, 15, 17.5, 20$, with $t_y/E_r = \frac{4}{\sqrt{\pi}}(V_y/E_r)^{3/4}e^{-2\sqrt{V_y/E_r}}$ [37]. Clearly, there is no obvious difference in the Leggett's bounds at the three temperatures. The superfluid fractions f_s^y computed via QMC winding number are also consistent with the case of $k_B T = 0.005E_r$, demonstrating the convergence of QMC calculations at sufficiently low temperatures.

Therefore, we conclude that the temperature $k_B T = 0.005E_r$ in the main text is low enough such that it reflects the zero-temperature properties of the superfluid fraction and Leggett's bound.

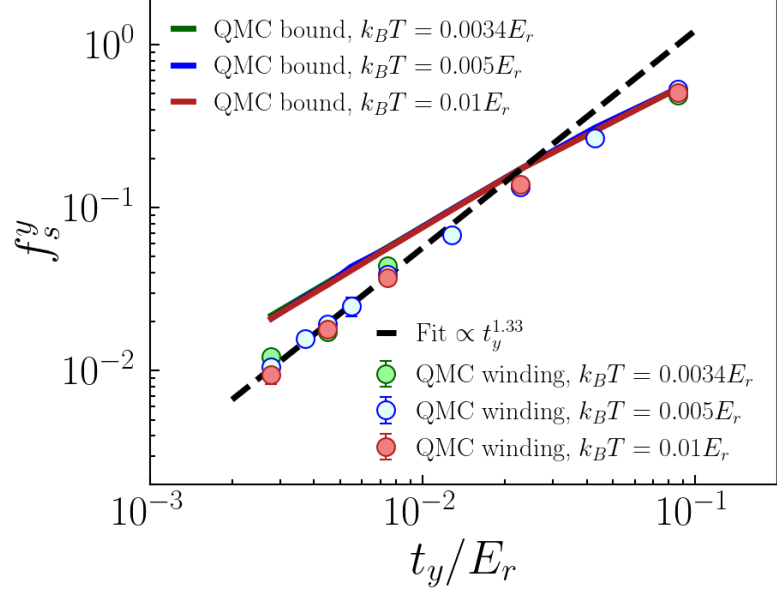


Figure S1. Comparison of QMC calculations for different temperatures $k_B T = 0.0034 E_r$ (green), $k_B T = 0.005 E_r$ (blue) and $k_B T = 0.01 E_r$ (red) in strong interaction regime $\tilde{g}_{2D} \simeq 1.364$, with the system size $L_x = 25a$, $L_y = 10a$. The solid lines are Leggett's bounds, with the linear fit in log-log scale of the superfluid fraction f_s^y (black dashed line) computed via QMC winding number at $k_B T = 0.005 E_r$ in the range $V_y \in [15, 20] E_r$ (blue circles).